

Drone-based Air Quality Monitoring: Development and Evaluation of Low-Cost PM_{2.5} Sensor for Remote Environmental Assessment

Mohd Shahrul Mohd Nadzir,^{1*} Utbah Rabuan,¹ Sawal Hamid Md Ali,² Jintu Borah,³
Shubhankar Majumdar,³ and Muhammad Saufy Rohmad⁴

¹Department of Earth Sciences and Environment, Faculty of Science and Technology,
Universiti Kebangsaan Malaysia, 43600 Bangi, Selangor, Malaysia

²Department of Electrical, Electronic and Systems Engineering, Faculty of Engineering and Built Environment,
Universiti Kebangsaan Malaysia, 43600 Bangi, Selangor, Malaysia

³Department of Electronics and Communication Engineering, National Institute of Technology Meghalaya,
Shillong 793003, India

⁴School of Electrical Engineering, Kompleks Kejuruteraan Tuanku Abdul Halim Mu'Adzam Shah,
Universiti Teknologi MARA, 40450, Shah Alam, Selangor, Malaysia

(Received December 19, 2024; accepted May 14, 2025)

Keywords: unmanned aerial vehicles (UAVs), low-cost air quality sensors (LCSs), particulate matters

Localized air pollution from open burning, waste disposal, and gas emissions remains difficult to monitor effectively, especially in inaccessible areas. Conventional air quality monitoring methods are often costly, stationary, and inadequate in coverage. We present AirborneSense, a novel unmanned aerial vehicle (UAV)-based monitoring system equipped with low-cost particulate matter (PM_{2.5}) sensors, GPS, and environmental sensors (temperature, humidity, and barometric pressure), using the Global System for Mobile Communications (GSM) to transmit real-time data to the cloud. The HPMA1115 PM_{2.5} sensor was chosen for its high accuracy, $R^2 > 0.7$, and a calibrated RMSE of 1.98, compliant with US EPA standards. Field tests were carried out at various altitudes and locations to evaluate system accuracy and adaptability. At higher altitudes, AirborneSense demonstrated its peak sensor performance with an R^2 value of 0.78, maintaining consistency with reference analyzers ($R^2 = 0.73$). The system effectively mapped pollution, revealing elevated PM concentrations in construction zones and significantly lower levels in rural areas. The findings underscore the potential of UAV-based systems to enhance spatial and temporal environmental assessments, providing a scalable, cost-effective tool for comprehensive pollution monitoring and management.

1. Introduction

Air pollution is a critical environmental issue affecting both public health and ecological balance worldwide. Rapid urbanization, industrial activities, and increased vehicular emissions have exacerbated the levels of harmful pollutants, particularly in densely populated areas.

*Corresponding author: e-mail: shahrulnadzir@ukm.edu.my
<https://doi.org/10.18494/SAM5449>

Among the various pollutants, particulate matter (PM), especially PM_{2.5}, poses a significant threat because of its ability to penetrate deep into the respiratory system,⁽¹⁾ thereby causing a range of health problems such as asthma,⁽¹⁾ cardiovascular diseases,⁽¹⁾ and even premature death.⁽¹⁾

Conventional air quality monitoring methods, including fixed air quality monitoring stations (FAQMSs), rely on stationary, high-cost, and maintenance-heavy equipment.^(2–6) While these systems offer precise data, they are limited by their fixed locations, resulting in inadequate spatial coverage, particularly in rural or hard-to-reach areas. Moreover, the deployment and operation of such systems can be financially prohibitive, especially in developing countries, where air quality issues are often more pronounced.

Recent advances in low-cost air quality sensors have opened new avenues for decentralized and real-time air quality monitoring.^(4–6) These sensors are portable, affordable, and easily deployable, making them a promising alternative to traditional monitoring networks.^(3,4) However, stationary sensor networks still face limitations in terms of spatial and temporal resolutions, particularly in dynamic environments such as construction zones, industrial areas, or during periods of open burning.

To address these limitations, the integration of unmanned aerial vehicles (UAVs), or drones, with air quality sensors has emerged as a novel approach.^(5,6) Drones offer enhanced mobility, allowing for the collection of data from multiple altitudes and locations, providing a more comprehensive understanding of pollution patterns. For example, a study by Bakirci⁽²⁾ introduced a drone-based system to systematically map NO₂, CO, PM₁₀, and PM_{2.5} around a torus-shaped building. The study revealed that pollutants were not uniformly distributed; instead, the inward facade of the building, compared with other areas, exhibited 12.64 to 15.77% higher pollutant concentrations. The findings demonstrated that building shape affects pollutant accumulation, leading to higher indoor air pollution in specific locations. This approach enables monitoring in areas that are otherwise inaccessible, offering the potential for the three-dimensional mapping of pollutants.^(2,6)

Recent advancements in UAV-based air quality monitoring have demonstrated their effectiveness in improving spatial coverage and pollution mapping^(2,6) evaluated the impact of UAVs on air quality management in smart cities, showing how drones enhance transportation-related pollution assessments. Similarly, studies by Lambey and Prasad⁽⁷⁾ and Bakirci⁽⁸⁾ explored the role of autonomous UAV networks in improving coverage and consistency in pollution mapping.⁽⁶⁾ These studies emphasize the growing role of UAVs in air quality research and support the approach taken in this study.

We introduce a newly developed UAV-based air quality monitoring system, known as AirborneSense, equipped with a low-cost PM_{2.5} sensor and environmental condition sensors (temperature, relative humidity, and barometric pressure). The system is designed to collect and transmit real-time data to the cloud via Global System for Mobile Communications (GSM) technology, enabling the remote monitoring of air pollution in diverse environments. Through extensive field tests and real-world applications, we demonstrate the effectiveness of AirborneSense in identifying pollution hotspots and providing detailed spatial and temporal pollution data.

By leveraging the capabilities of drone technology and advanced sensors, in this research, we aim to contribute to the development of more efficient, scalable, and accessible air quality monitoring solutions, particularly in regions with limited resources. The findings of this study underscore the potential of drone-assisted air quality monitoring in advancing environmental management and public health protection.

2. Research Methodology

2.1 Low-cost air quality sensor (LAQS)

The electrochemical sensor used in this experiment was developed to target various toxic gases, prioritizing increased sensitivity, reduced power consumption, compact design, and cost-effectiveness.^(3,9,10) The sensor's performance relies on an amplifier circuit, which accurately measures small fluctuating currents and converts them into a corresponding voltage signal (millivolts, mV). This analog signal is then processed digitally via the I2C protocol, producing concentration units such as parts per billion (ppb) or micrograms per cubic meter ($\mu\text{g}/\text{m}^3$).

To ensure accurate location tracking, the sensor data is combined with GPS-derived latitude and longitude coordinates, as well as altitude data from an altitude sensor. This dataset is transmitted via General Packet Radio Service (GPRS) to a remote server for real-time visualization or historical analysis, enabling the generation of three-dimensional air quality maps. This integrated system, called AirborneSense, allows for dynamic and comprehensive air quality monitoring. The detailed calibration for $\text{PM}_{2.5}$ and PM_{10} is described in Ref. 9.

2.2 Hardware design

AirborneSense was developed for autonomous, long-term operation with minimal maintenance, as illustrated in Fig. 1. At its core, the system is powered by the ESP32-TTGo T-Call microcontroller unit (MCU), which manages all software protocols to ensure comprehensive system functionality. The design includes five primary components: the sensing unit, positioning unit, processing and integration unit, transmission unit, and power supply. The various sensors can be assembled with AirborneSense to measure the concentrations of nitrogen dioxide (NO_2), sulphur dioxide (SO_2), ozone (O_3), and carbon monoxide (CO). However, in this study, we focused mainly on $\text{PM}_{2.5}$ measurement.

To safeguard sensor readings from wind interference caused by the drone's propellers, a specially designed enclosure with a vent system was integrated. This setup enables controlled airflow and minimizes external disturbances. Additionally, a durable mounting plate was created to secure the system to the drone and mitigate vibration-induced voltage fluctuations, enhancing data precision. Both the mounting plate and the enclosure are made from the ABS material to ensure long-lasting durability.

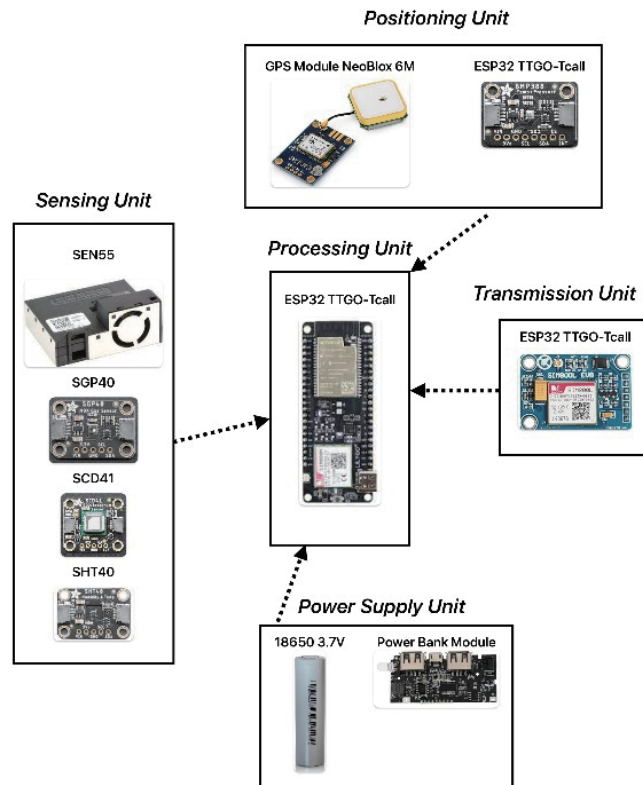


Fig. 1. (Color online) AirborneSense hardware architecture.

2.2.1 MCU

ESP32 TTGO T-Call was selected as the main MCU for the AirborneSense prototype because of its affordability (approximately USD 12) and robust feature set. Produced by LilyGO, this board includes 34 pinouts, two I2C interfaces, two SPI interfaces, three UART interfaces, and 34 GPIO pins, making it well suited for this project.

Serving as the system's central processing unit, the MCU runs the Arduino code to control the various integrated modules such as sensors, GPS, and GPRS. It collects pollutant concentration data from the sensors and combines this information with GPS coordinates and altitude measurements. The complete dataset is then transmitted to the cloud via the SIM800L module, enabling real-time monitoring.

2.2.2 Printed circuit board (PCB) design

It is crucial to use connectors with strong antivibration specifications because the prototype sensor is attached to a flying drone. The aim of this precautionary measure is to stop any unintentional connector disconnection or breakage during flight brought on by the vibrations of the drone. A specific PCB was created to satisfy this requirement while adhering to industry standards. EasyEDA, a CAD design program, was used to carry out the design process. The connector layout depicted in Fig. 2 was designed to establish firm and reliable connections. This



Fig. 2. (Color online) PCB used in this study.

design minimizes the risk of the connector disengaging from the socket during flight. The design was then sent to JLCPCB, a reputable PCB fabrication company, in accordance with the requirements stated in the IEC453645 standard, so that it could be fabricated.

The PCB incorporates a voltage regulator circuit, which plays a vital role in ensuring the proper operation of the sensors that have been attached to the prototype of AirborneSense. These sensors typically require a stable voltage of 3.3 or 5 V to function optimally. By receiving a 5 V input from the power source, the voltage regulator effectively regulates and converts it into a stable 3.3 V output, which is then supplied to the sensors. The dimensions of the PCB are designed to match those of the MCU, taking into account size constraints. With a weight of just 10 g, the PCB constitutes approximately 5% of the total weight of the entire prototype of AirborneSense.

2.3 Sensing unit

We also aim to understand how environmental conditions, such as temperature and humidity, affect PM and sensor readings. The sensors selected were chosen for their effectiveness in outdoor applications, focusing on accurate pollutant concentration detection while ensuring stability under varying environmental conditions and airspeeds due to the drone's propellers. For PM_{2.5} detection, the SEN55 sensor was selected because of its durability and adaptability. Its compact dimensions (52.8 × 43.6 × 22.3 mm³) make it a suitable fit for the AirborneSense prototype.

The SEN55 sensor provides integrated measurements of PM, volatile organic compounds (VOCs), NO_x, temperature, and relative humidity (RH). It features a digital output to reduce interference and communicates via the I2C protocol. Operating at 5 V with a peak current of 5 mA, the sensor draws air through its chamber, where particles are detected using a laser and photodiode. This process converts particle data into digital signals that are then processed by the MCU.

2.4 Position unit

To improve the understanding of pollutant sources in three-dimensional space, AirborneSense integrates a GPS module and a barometric/altitude sensor. The GPS provides latitude (x -axis) and longitude (y -axis) data, while the barometric sensor adds altitude (z -axis) information. By combining these measurements, we generate a 3D dataset that enables the creation of detailed air quality profiles, allowing for the precise identification of pollution sources, unlike traditional methods that lack positional data integration.

To obtain height data for 3D air quality mapping, the AirborneSense system integrates the Bosch BMP388 barometric sensor. This sensor provides highly accurate altitude measurements, with a relative accuracy of ± 8 Pa (equivalent to ± 0.5 meters) and an absolute accuracy within ± 50 Pa. It also features an integrated temperature sensor with an accuracy of ± 0.5 °C across a range of 0 to 65 °C. Communication with the MCU is facilitated through the I2C protocol and enhanced with a cyclic redundancy check (CRC) checksum for data integrity. The sensor is designed using the STEMMA QT standard for seamless integration with the system.

To improve the understanding of pollutant sources in three-dimensional space, AirborneSense integrates a NEO-6M GPS module and a BMP388 barometric/altitude sensor. The NEO-6M GPS module determines latitude (x -axis) and longitude (y -axis) coordinates using signals from at least three satellites, offering a manufacturer-specified horizontal positional accuracy of 2.5 m under optimal satellite visibility conditions. However, to validate this claim, we performed independent field calibration tests by placing the GPS module at a fixed reference location with known coordinates and comparing its readings against a high-precision geodetic GPS (± 0.1 m accuracy). The results showed that in open areas with minimal obstructions, the mean positional error ranged from 2.3 to 2.8 m, which aligns well with the manufacturer's specifications.

In urban environments, where multipath interference and satellite occlusion are more significant, the positional error increased to approximately 3.5 to 4.2 m in some instances. These variations were accounted for in post-processing using GPS data smoothing techniques, ensuring that mapping inconsistencies were minimized. Additionally, to enhance spatial accuracy, we incorporated barometric altitude corrections from the BMP388 sensor, which provides a relative accuracy of ± 0.5 m. The altitude readings were cross-validated with reference data from a drone flight controller system. While the current setup provides reasonably accurate location data for pollution mapping, future improvements may involve real-time kinematic (RTK) GPS integration, which could enhance horizontal accuracy to submeter levels for even more precise air pollution geospatial assessments.

2.5 Transmission unit

The AirborneSense prototype employs the SIM800L module by SIMCOM to transmit data to the cloud over a 2G network. Operating on GSM technology, the module connects to internet service providers (ISPs) through GPRS. Powered by a stable 3.7 V source, it communicates using the UART protocol with a baud rate of 9600, ensuring reliable data transfer.

For network connectivity, the system uses a SIM card from Celcom, a Malaysian telecommunications provider. The SIM800L module, utilizing AT commands, establishes a 2G connection that allows the secure, continuous transmission of air quality data to the cloud, enabling real-time monitoring and analysis. A GPRS-optimized antenna was selected to ensure effective communication, as GPRS-specific antennas are essential for this module's operation.

2.6 Power supply unit

The AirborneSense prototype is powered by a 18650-type lithium-ion battery with a nominal voltage of 3.7 V and a capacity of 3500 mAh, supplying ample power for operation. This battery can support up to 15 A of surge current, ensuring reliable performance during periods of peak demand. Connected to a power bank module, the battery benefits from integrated circuits for power protection, battery charging, and voltage regulation. The protection circuit safeguards against overcurrent and reverse polarity, while the charging circuit stabilizes voltage during charging, preserving battery health.

The power regulation circuit outputs a consistent 5 V to power the prototype's components. A USB Type-C cable connects the power bank module to the PCB, where the 5 V output is further regulated down to a stable 3.3 V to power most sensors. During normal operation, the system typically draws 300 mA with a maximum demand of 2 A during data transmission.

2.7 Code and communication flow

The MCU serves as the central control unit of the AirborneSense system, similar to a motherboard, and operates using an Arduino code script. The script's execution flow is illustrated in a flowchart (Fig. 3), showing the step-by-step process and decision points. The code initializes the SIM800L module for communication, with necessary libraries (e.g., "TinyGSM", "TinyGPS", and "SEN55") loaded for GPS data processing, environmental sensing, and other key operations.

Pin assignments (Table 1) are set to ensure proper communication between the MCU and components. The SIM card settings, including the access point name (APN) for the telecommunication provider, are initialized to establish internet connectivity. Data transmission to the Thingspeak server is facilitated via an API, which securely sends air quality data, GPS coordinates, and other variables.

Every 20 s, the system retrieves sensor data (e.g., temperature, humidity, GPS location, PM_{2.5}, VOC concentration, and CO₂ level) and organizes it in JSON format. Before data transmission, the code checks for an active GPRS connection. If not connected, it re-establishes the connection with the Celcom network. Once the connection is verified, data is sent to the ThingSpeak server by the HTTP POST method.

2.8 Transmission architecture of AirborneSense

AirborneSense utilizes a GPRS data network (Celcom) for transmitting sensor data to the cloud via HTTP. ThingSpeak is the chosen cloud storage platform because of its real-time data

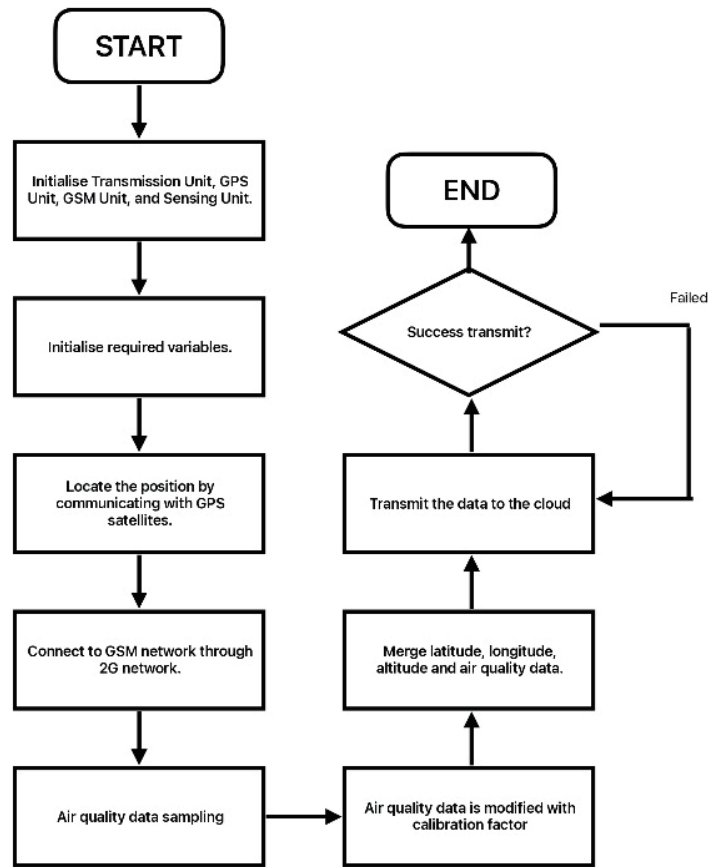


Fig. 3. Communication flow for *AirborneSense*.

Table 1
Pin assignment for electronic module.

Modules	Module Pin	MCU Pin
BMP388	I2C SDA	32
	I2C SCL	33
SEN55	RXD	18
	TXD	19
SCD41	I2C SDA	21
	I2C SCL	22
SGP40	I2C SDA	17
	I2C SCL	16

collection, processing, graphical representation, and seamless integration with MATLAB for analysis.

Figure 4 outlines the cloud data processing flow. ThingSpeak’s channel system is used to store and organize data, with each channel having eight fields and three location fields. In this study, one channel is used: Field 1 records temperature, Field 2 records relative humidity (RH), Field 3 stores latitude, Field 4 stores longitude, Field 5 records height, Field 6 captures PM_{2.5}

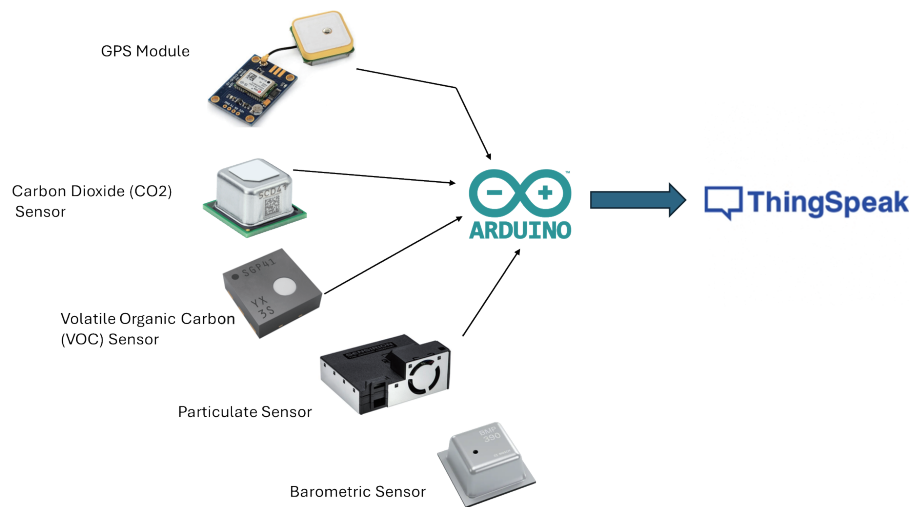


Fig. 4. (Color online) Flow of data transmission.

levels, Field 7 denotes VOC concentration, and Field 8 represents CO₂ level. Although capable of measuring additional pollutants such as PM₁₀ and NO_x, in this study, we focus on PM_{2.5}, VOCs, and CO₂.

ThingSpeak operates through a REST API, transmitting data in JSON format, and requires a channel ID and API key for data access and control. The write API key is used for data submission, while the read API key allows retrieval from anywhere in the world, reducing maintenance costs and simplifying network management. ThingSpeak also provides the graphical visualization of stored data, automatically updating fields at predefined intervals. This feature helps monitor data transmission and detect abnormalities, triggering evaluations when issues arise.

2.9 Outdoor testing

Two types of analyses were performed on the AirborneSense system under real outdoor conditions: vertical ascent accuracy and performance at a fixed location.

2.9.1 Vertical hovering test

The vertical accuracy test was conducted on January 20, 2023, during a one-day experiment. The test took place at the Faculty of Engineering, Universiti Teknologi Mara (UiTM) Shah Alam campus (see Fig. 5); the faculty's building has 21 floors, which provided an ideal environment for the experiment. A TOPAS, a reference analyser for PM_{2.5}, was placed on the ground, 6th, 13th, 16th, and 21st floors, and the AirborneSense drone flew alongside these levels, maintaining a consistent distance of 5 m from the TOPAS units for synchronized measurements. The drone was operated for 14 min at each level, in line with the battery's operational limit, while TOPAS units recorded data simultaneously for accurate comparison. Data from each floor were averaged



Fig. 5. (Color online) (a) & (b) Experimental setup at UiTM Shah Alam (arrow indicates drone's position).

and compared between AirborneSense and TOPAS to calculate the R^2 correlation, assessing the accuracy of the $PM_{2.5}$ measurements obtained using the LAQS drone and the effect of altitude on sensor accuracy. The results provided insights into the correlation between sensor readings and environmental conditions at various altitudes.

2.9.2 Fixed position hovering test

The performance of the AirborneSense drone in the static flight mode was assessed between April 9th and May 10th, 2023, during the west monsoon season. The test was conducted in a rural area to ensure safety and minimize interference from urban pollution. The location, characterized by natural greenery and scattered houses, provided an ideal environment for accurate data collection.

The TOPAS device at ground level was installed near a stable power source, while AirborneSense was flown 5 m away at a height of 10 m to prevent propeller-induced airflow from affecting the TOPAS readings. Each flight session lasted 10 min, constrained by the drone's battery capacity. Data were collected twice daily: once in the morning (9–11 am) to capture vehicular emissions and once in the evening (4–6:30 pm) to detect pollutants from residential activities.

Data from both AirborneSense and TOPAS were averaged and compared, with the R^2 correlation coefficient calculated to assess the drone's performance under various environmental conditions. This experiment was crucial for understanding the accuracy of AirborneSense under real-world field conditions, as external factors such as propeller airflow can introduce turbulence that affects pollutant measurements.

2.9.3 Field hovering test

On July 1, 2023, a single-day field test using the AirborneSense drone was conducted to evaluate its performance in real-time air quality mapping under real-world conditions. The aim of this test was to verify the system's reliability and accuracy during field deployment.

Because of budgetary and time constraints, the experiment was condensed into two days, focusing on gathering detailed, location-specific air quality data. Test sites included rural, semirural, and newly developed township areas, as depicted in Fig. 6 and listed in Table 2. Despite the limitations, the field test provided valuable insights into the drone's capability to deliver dependable air quality data across varied environments.

3. Results and Discussion

3.1 Airbornesense testing in a real environment

In this section, we will explore the data reliability collected by AirborneSense under real-world conditions. Initially, a series of test flights at varying altitudes were performed to assess how height affects the precision of air quality measurements captured by AirborneSense. Following this, a stationary test was conducted to evaluate the correlation between AirborneSense data and environmental parameters, thereby assessing the system's accuracy.



Fig. 6. (Color online) Selected sampling areas at Universiti Kebangsaan Malaysia campus.

Table 2
Location of interest for data sampling.

No.	Location	Type of Location
1	Dewan Gemilang UKM	Semirural
2	Setia Alam Sari Housing Area	Construction area
3	UKM Reservation Forest	Forest reserve
4	Bangunan FST UKM	Semirural

Lastly, AirborneSense underwent a comprehensive real-environment test flight spanning an entire day, without the support of any reference analyzers. This phase was aimed at evaluating the reliability of AirborneSense and its ability to identify pollution sources by comparing its data with the results of ground-based measurements.

3.2 Test-flight in multiple height

Figures 7(a)–7(e) and Table 3 show the outcomes of test flights conducted at assorted altitudes and present a clear linear progression between the altitude at which AirborneSense operates and the exactitude of its air quality measurements. With each elevation increment of roughly 15 m, there is a notable boost in R^2 , which intriguingly shows a doubling of the previous value. This enhancement in R^2 is consistent even as higher altitudes reveal lower $PM_{2.5}$ concentrations, suggesting the robustness of the AirborneSense system across different altitudes.

The results of the study's initial phase at the ground level indicated a subpar R^2 value, which did not meet the US EPA's benchmark for accuracy. Yet, as the drone ascended, surpassing the height of the surrounding buildings, R^2 improved, attaining a maximum of 0.77, which is within the acceptable range per US EPA standards. We posit that environmental conditions at increased altitudes, such as the diminished interference from the ground level and the uniformity of air masses, substantially enhance sensor performance.

Moreover, when the drone hovered at the first level, the generated airflow from the propellers, coupled with the confinements of a fully constructed area, resulted in an unpredictable air movement. This phenomenon, coupled with the drone's proximity to building structures that disrupted the airflow, likely led to the diminished R^2 observed during lower altitude flights.

Considering the above findings, altitude emerges as a pivotal element in air quality monitoring strategies, underscoring the importance of selecting an appropriate environment for data collection. The potential of drones, particularly those with calibrated sensors such as AirborneSense, is highlighted as they provide valuable data for environmental monitoring, aiding in the rapid identification of areas of concern. Future studies should delve into the dynamics between advancements in sensor technology and environmental conditions at various altitudes to further refine methodologies for air quality assessment.

3.2.1 Test flight in fixed coordinates

In the conducted study, AirborneSense was deployed at a fixed height of approximately 20 m above ground level at fixed latitude and longitude to collocate $PM_{2.5}$ concentrations in a rural setting characterized by widely spaced houses, abundant tree cover, and minimal human activity. This approach facilitated the collection of air quality data over a one-month period, after which a collocation analysis with data from a reference analyzer was performed.

Figure 8 highlights that the minimal $PM_{2.5}$ concentration detected by the reference analyzer was $0.08 \mu\text{g}/\text{m}^3$, while the drone's sensors reported a minimum of $4.2 \mu\text{g}/\text{m}^3$. On the upper end of the spectrum, the reference analyzer's measurements topped at $24.38 \mu\text{g}/\text{m}^3$, compared with the drone's substantially higher peak measurement of $89.4 \mu\text{g}/\text{m}^3$. The resulting R^2 stands at

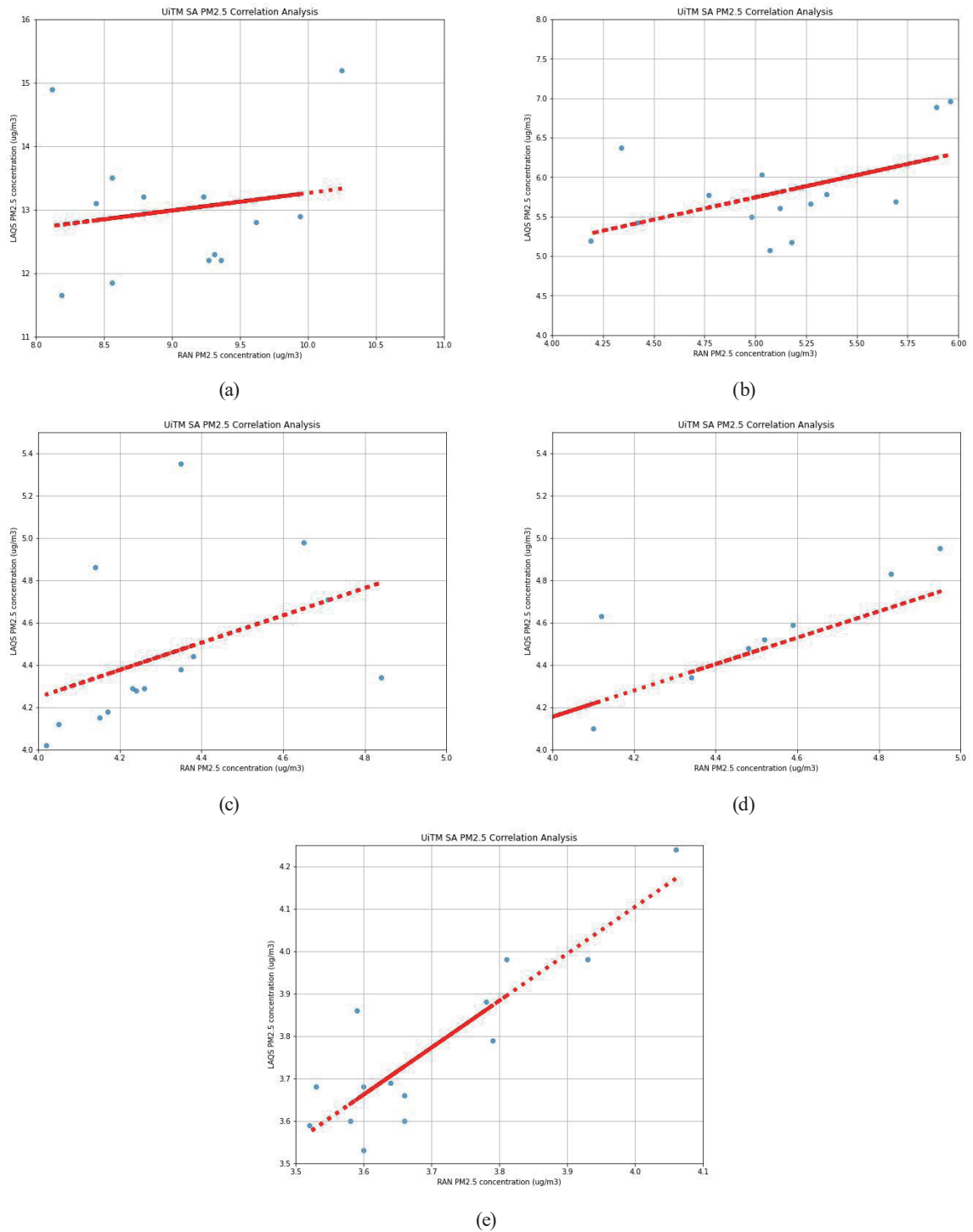


Fig. 7. (Color online) Correlation of AirborneSense and Reference instruments at different levels: (a) level 1, (b) level 6, (c) level 13, (d) level 16, and (e) level 21.

Table 3

Results of statistical evaluation between AirborneSense and reference PM_{2.5} measurements.

Floor Level	Altitude (m)	R^2	Standard deviation (TOPAS)	Standard deviation (AirborneSense)	p -value
1	1	0.033	0.696	0.894	<0.01
6	25	0.268	0.541	0.663	<0.01
13	40	0.177	0.248	0.347	<0.01
16	50	0.424	0.370	0.355	<0.01
21	65	0.775	0.158	0.198	<0.01

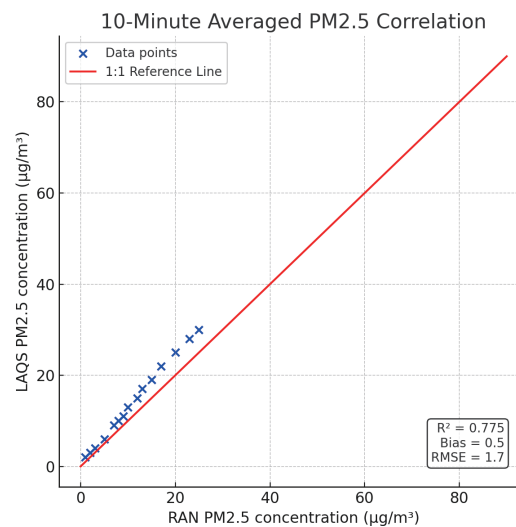


Fig. 8. (Color online) Correlation of results obtained from AirborneSense and reference instrument in rural area.

0.73, reflecting a robust correlation between the measurements obtained from the drone and those from the reference analyzer. In accordance with the standards set forth by the US EPA, an R^2 value exceeding 0.7 denotes a high sensor reliability in air quality measurement. This notable result underscores the utility and reliability of drone technology in monitoring air quality, particularly in less urbanized areas.

Firstly, the high R^2 value underscores the reliability and accuracy of drone-based sensors in capturing PM_{2.5} concentrations, even in areas with lower pollution levels and less anthropogenic activity. The results showed a good correlation between the UAV-based system and reference instruments, with R^2 values above 0.7, demonstrating the reliability of the system. However, some extreme variations were observed in the measurements, particularly in certain high-concentration periods. These anomalies may be attributed to several factors, including environmental effects, sensor response time, calibration limitations, and meteorological conditions:

- (1) Environmental effects – Variability in pollutant concentration due to localized emission sources (e.g., vehicular emissions, industrial activity, and open burning) may cause temporary spikes or drops in readings.
- (2) Sensor response time – Low-cost sensors have short response delays compared with reference-grade instruments, which may lead to inconsistencies when measuring sudden changes in pollutant levels.⁽³⁾

- (3) Calibration limitations – Although sensor calibration was performed, temperature, humidity, and cross-sensitivity to other gases could introduce deviations in real-world conditions especially tropical countries such as Malaysia.^(3,9,10)
- (4) Meteorological conditions – Wind speed and direction play a crucial role in pollutant dispersion. Rapid changes in airflow dynamics may result in inconsistencies between stationary and drone-based measurements.^(11–14)

Despite these variations, the overall correlation remains strong ($R^2 > 0.7$), demonstrating the effectiveness of the UAV-based system in monitoring air quality. Further refinements in sensor placement, response-time correction, and advanced calibration models may help reduce these discrepancies in future studies.

Challenges encountered during the data collection, such as variable wind conditions and atmospheric stability, may have affected the drone's sensor readings.^(15–17) Future studies should be aimed at the control of these variables or the use of a larger fleet of drones to validate the findings presented here. Moreover, incorporating more diverse urban environments and a range of building heights could further clarify the impact of built structures on air quality.

In Fig. 8, a detailed comparison between AirborneSense and the reference instrument is shown. The figure includes a 1:1 reference line to represent an ideal agreement, along with RMSE and bias values to quantify discrepancies. Confidence intervals are also included to visualize variability in measurement. The results show a moderate level of agreement, with some deviations attributed to sensor drift, atmospheric turbulence, and short-term variability in $PM_{2.5}$ concentration. These factors are consistent with trends observed in previous figures and support the reliability of the AirborneSense platform, especially at higher altitudes.

3.2.2 Flight test in a real environment

We evaluated the AirborneSense drone's ability to identify pollution sources by measuring $PM_{2.5}$ concentrations, integrating geographical coordinates, and assessing the environmental conditions at each site. Four distinct locations, spaced 3 km apart, were chosen to determine the system's sensitivity to spatial variations in air quality.

Figure 9 reveals that the highest average $PM_{2.5}$ concentration ($7.01 \mu\text{g}/\text{m}^3$) was observed at site 2, while the lowest concentration ($2.74 \mu\text{g}/\text{m}^3$) was recorded at site 3. Sites 1 and 4 exhibited similar average concentrations of $3.15 \mu\text{g}/\text{m}^3$ and $3.24 \mu\text{g}/\text{m}^3$, respectively. In the absence of a ground-based reference analyzer, the validation of these measurements relied solely on observational assessments of each location.

Further analysis, as depicted in Fig. 10, indicates that site 2, an active construction zone for residential development, exhibited the highest $PM_{2.5}$ concentration. This elevation in $PM_{2.5}$ concentration could be directly attributed to local construction activities, including soil excavation, transportation, and asphalt application, which are known to significantly contribute to airborne particulate concentrations. A comparative analysis with a study conducted in a construction zone revealed a ground-level $PM_{2.5}$ concentration of $79.85 \mu\text{g}/\text{m}^3$. This figure starkly contrasts with the readings obtained from AirborneSense, which underestimated the $PM_{2.5}$ concentrations by a factor of 10 compared with the ground measurements. This discrepancy aligns with findings in other research, which indicated that the vertical dispersion of



Fig. 9. (Color online) Sites chosen for air quality profiling. Note: differences between site altitudes were minimal (within ± 3 km).



Fig. 10.. (Color online) Site 2 conditions.

PM_{2.5} occurs as particles move away from their source.^(17,18) Additionally, these studies corroborate the observation that there is a significant correlation between the vertical concentration of PM_{2.5}, particularly its maximum level, and the surface concentration of PM_{2.5}. This correlation suggests that surface PM_{2.5} measurements can be effectively utilized to predict the vertical PM_{2.5} concentration distribution.

The analysis revealed that sites 1 and 4 exhibit intermediate PM_{2.5} concentrations compared with sites 2 and 3. Observational data, including on-site inspections and aerial imagery, indicated minimal local activities at these sites, such as sports (football and golf), few buildings, and recreational engagements, suggesting that these locations themselves are not significant sources

of $PM_{2.5}$. Instead, the predominant contribution to $PM_{2.5}$ concentrations at these sites was likely due to their proximity to major roadways, located less than 2 km away. Specifically, site 1 is situated to the south of Jalan Bangi-Reko and site 4 is located to the east of Lebuhraya Utara-Selatan. Both roads have high traffic volumes, particularly during morning and evening peak hours, which is a notable factor in urban $PM_{2.5}$ pollution.

Vehicular emissions are identified as a primary source of $PM_{2.5}$ in urban settings.⁽¹⁸⁾ These emissions encompass not only $PM_{2.5}$ but also other pollutants such as NO_2 , SO_2 , VOCs, and CO, which is a key indicator of incomplete combustion in vehicle engines. However, this study focuses exclusively on $PM_{2.5}$, and other vehicular pollutants were not measured. These substances can react with the atmosphere to form secondary PM, further exacerbating air quality issues. The proximity of sites 1 and 4 to such busy thoroughfares underscores the effect of vehicular traffic on local $PM_{2.5}$ levels. Despite the low level of direct anthropogenic activities at these sites, the significant impact of nearby road traffic on air quality highlights the need for comprehensive urban air quality management strategies that address vehicular emissions as a central concern.

This discussion aligns with existing literature indicating that road traffic is a critical contributor to urban PM pollution.⁽¹⁸⁾ It emphasizes the importance of integrating traffic management and urban planning efforts to mitigate the impact of vehicular emissions on air quality. Furthermore, it supports the adoption of cleaner transportation options and the enhancement of monitoring and regulatory frameworks to control urban air pollution effectively.

Site 3 exhibited the lowest $PM_{2.5}$ level, indicating that it neither serves as a pollution source nor is proximate to high-activity areas. Its location, characterized by a considerable distance from busy roads and the absence of major construction, is in a secluded area with sparse human activity, adjacent to forested land. This direct observation highlights a clear link between the extent of human activity and $PM_{2.5}$ concentration, affirming the critical role that anthropogenic factors play in affecting air quality.

The results of our study not only validate the effectiveness of the AirborneSense drone in detailed air quality monitoring but also emphasize the significant role that local sources play in the variability in $PM_{2.5}$ level. They support the adoption of UAV technology in environmental evaluations and offer a fresh viewpoint on how pollutants and their origins are spatially distributed. Utilizing the AirborneSense drone enables the development of precise air pollution profiles by flying over targeted areas of interest. This approach could greatly assist authorities in identifying pollution hotspots by deploying the AirborneSense drone for surveillance.

For future research directions, it is recommended to pair the drone with ground-based reference analyzers for validation purposes and to extend the investigation across a wider range of environmental scenarios. Such enhancements would improve the depth and accuracy of air quality mappings and provide valuable insights into effective pollution management strategies.

4. Conclusions

In this study, we demonstrated the feasibility and effectiveness of integrating drone technology with the LAQS system for real-time environmental monitoring, specifically focusing on $PM_{2.5}$ measurements. The comprehensive tests—spanning varying altitudes, fixed locations,

and different environments—showed that drone-assisted air quality monitoring can provide accurate, location-specific data. A significant linear relationship between altitude and PM_{2.5} measurement accuracy was observed, with higher altitudes offering clearer profiles of atmospheric pollutants.

In fixed-position tests, the AirborneSense drone reliably captured spatial variations in PM_{2.5} level with a strong R^2 correlation (0.73) between drone and reference measurements, particularly in rural settings. The drone effectively identified localized pollution sources, such as construction and vehicular activity, underscoring its utility in targeted environmental management.

While this study successfully demonstrates the feasibility of UAV-based PM_{2.5} monitoring, several limitations should be acknowledged. These include the use of a single low-cost sensor, which may experience accuracy drift due to environmental factors such as humidity and temperature; the exclusive focus on PM_{2.5}, without accounting for other key pollutants such as NO₂, CO, and VOCs; and limited spatial-temporal coverage due to UAV battery constraints. Additionally, external factors such as wind and turbulence may affect the consistency of measurements. Future work should consider integrating multi-pollutant sensor systems, adopting real-time calibration strategies, expanding flight coverage through autonomous UAV networks, and incorporating meteorological modeling to improve pollutant dispersion analysis.

In conclusion, the AirborneSense drone system offers a novel, versatile approach for air quality monitoring across diverse locations and altitudes, providing valuable insights into pollution dynamics. While promising, further refinement—particularly in long-term data collection, calibration techniques, and mitigating the impact of propeller airflow—will enhance its accuracy and broaden its application in safeguarding public health and the environment.

Acknowledgments

We would like to thank The Collaborative Research in Engineering, Science and Technology Centre (CREST) registered at Universiti Kebangsaan Malaysia (UKM) for their support through grant number CREST-2021-001. Dr. Shubhankar Majumdar would like to thank ASEAN INDIA S&T DEVELOPMENT FUND (AISTDF) for their support through grant number CRD/2020/000320. Finally, we would like to thank Dr. Sakinah Mohd Alauddin for her support and assistance in obtaining permission to conduct drone flights at Tower 2, Faculty of Chemical Engineering, Universiti Teknologi MARA (UiTM). This permission was crucial for carrying out the altitude-based measurements essential to this study.

References

- 1 A. Alias, M. S. Mohd Nadzir, M.T. Latif, M. F. Khan, H. H. Abd Hamid, M. Sahani, M. I. A. Wahab, M. Othman, F. Mohamed, N. Mohamad, N. Amil, and O. M. Kolapo: *Air Qual. Atmos. Health* **17** (2021) 1.
- 2 M. Bakirci: *J. Build. Eng.* **87** (2024) 109023. <https://doi.org/10.1016/j.jobe.2024.109023>
- 3 K. M. Alhasa, M. S. Mohd Nadzir, P. Olalekan, M. T. Latif, Y. Yusup, M. R. Faruque, F. Ahamad, H. H. A. Hamid, K. Aiyub, S. H. Md Ali, M. F. Khan, A. Abu Samah, I. Yusuff, M. Othman, T. M. F. Tengku Hassim, and N. E. Ezani: *Sensors* **18** (2018) 4380. <https://doi.org/10.3390/s18124380>

- 4 Z. H. Chen, B. W. Li, B. Li, Z. R. Peng, H. C. Huang, J. Q. Wu, and H. D. He: *Environ. Pollut.* **348** (2024) 123893. <https://doi.org/10.1016/j.envpol.2024.123893>
- 5 Z. Li, J. C. H. Fung, and A. K. H. Lau: *Build. Environ.* **143** (2018) 196. <https://doi.org/10.1016/j.buildenv.2018.07.014>
- 6 D. J. Miller, B. Actkinson, L. Padilla, R. J. Gri, K. Moore, P. G. T. Lewis, and S. P. Hamburg: *Env. Sci. Technol.* **54**. (2020) 2133. <https://doi.org/10.1021/acs.est.9b05523>
- 7 V. Lambey and A. Prasad: *Water Air Soil Pollut.* **232** (2021) 1.
- 8 M. Bakirci: *Sustain Cities Soc.* **106** (2024) 105390.
- 9 U. Rabuan, M. S. Mohd Nadzir, S. Z. Abdullah Sham, S. B. I. Wan Shaiful Bahri, S, J. Borah, S. Majumdar, T. M. T. Lei, S. H. Md Ali, M. I. A. Wahab, and N. H. Mohd Yunus: *Sens. Mater.* **35** (2023) 2881. <https://doi.org/10.18494/SAM4393>
- 10 Z. Khaslan, M. S. Mohd Nadzir, H. Johar, Z. Siqi, N. A. Sulong, F. Mohamed, S. Majumdar, F. N. A. Suris, N. S. S. L. Hawari, J. Borah, M. O. C. Gee, M. I. A. Wahab, and M. A. A. Bakar: *Water Air Soil Pollut.* **235** (2024) 2.
- 11 H. N. K. Vu, Q. P. Ha, D. H. Nguyen, T. T. T. Nguyen, T. T. Nguyen, T. T. H. Nguyen, N. D. Tran, and B. Q. Ho: *Atmosphere* **11** (2020) 750.
- 12 M. S. Mohd Nadzir, M. C. G. Ooi, K. M. Alhasa, M. A. A. Bakar, A. A. A. Mohtar, M. F. F. M. Nor, M. T. Latif, H. H. A. Hamid, S. H. M. Ali, N. M. Ariff, J. Anuar, F. Ahamad, A. Azhari, N. M. Hanif, M. A. Subhi, M. Othman, and M. Z. M. Nor: *Aerosol Air Qual. Res.* **20** (2020) 1237. <https://doi.org/10.4209/aaqr.2020.04.0163>
- 13 M. S. Mohd Nadzir, M. Z. Mohd Nor, M. F. F. Mohd Nor, M. I. A. Wahab, S. H. M. Ali, M. K. Otuyo, M. A. Abu Bakar, L. H. Saw, S. Majumdar, M. C. G. Ooi, F. Mohamed, B. A. Hisham, H. H. Abd Hamid, Z. Khaslan, N. Mohd Ariff, J. Anuar, G. R. Tok, N. A. Ya'akop, and M. Mohd Meswan: *Sustainability* **13** (2021) 12217. <https://doi.org/10.3390/su132112217>
- 14 H. Khreis, J. Johnson, K. Jack, B. Dadashova, and E. S. Park: *Int. J. Environ. Res. Public Health* **19** (2022) 1647. <https://doi.org/10.3390/ijerph19031647>
- 15 M. Bakirci: *Sci. Total Environ.* **909** (2024) 168606. <https://doi.org/10.1016/j.scitotenv.2023.168606>
- 16 V. Lambey and A. Prasad: *Water Air Soil Pollut.* **232** (2021) 1.
- 17 R.-F. Song, D. -S. Wang, X.-B. Li, B. Li, and Z.-R. Peng: *Atmos. Environ.* **265** (2021) 118724.
- 18 M. S. Mohd Nadzir, M. C. G. Ooi, K. M. Alhasa, M. A. A. Bakar, A. A. A. Mohtar, M. F. F. M. Nor, M. T. Latif, H. H. A. Hamid, S. H. M. Ali, N. M. Ariff, J. Anuar, F. Ahamad, A. Azhari, N. M. Hanif, M. A. Subhi, M. Othman, and M. Z. M. Nor: *Aerosol Air Qual. Res.* **20** (2020) 1237. <https://doi.org/10.4209/aaqr.2020.04.0163>